CHAPTER VI

Thermal Diffusion and Magneto Hydrodynamic Effects on Heat and Mass Transfer of Steady, Viscous Incompressible, Electrically Conducting Fluid in a Rotating Disk Embedded in a Porous Medium

6.1 Introduction

In Fluid Mechanics, the study of heat and mass transfer of an electrically conducting fluid due to a rotating disk embedded in a porous medium plays a vital role due to its applications in many areas such as oceanography, rotating machinery, computer storage devices, geophysical and geothermal engineering, porous heat exchangers, etc. Because of its industrial applications, the problem of heat and mass transfer due to rotating disk embedded in a porous medium in the presence of magnetic field has been the subject of many experimental and analytical studies.

Von Karman (1921) studied the hydrodynamic steady flow problem due to an infinite rotating disk using similarity transformations to reduce the partial differential equations into ordinary differential equations. Cochran (1934) obtained the asymptotic solutions for the steady flows past a rotating disk.

Benton (1966) developed Cochran's (1934) solutions to solve the unsteady problems. Miklavcic and Wang (2004) extended Von Karman's problem by studying the effects of slip where the surface of the rotating disk admits partial slip.

Stuart (1954) studied the effect of suction on the steady flow due to a rotating disk. Sparrow and Gregg (1960) studied the effect of Prandtl number on steady state heat transfer due to a rotating disk at a constant temperature. Compressible laminar flow and heat transfer about a rotating disk was studied by Ostrach and Thornton (1958).

Effect of an external uniform magnetic field on the flow due to a rotating disk was studied by Attia (1995). Later Attia (2009) studied the steady flow of an incompressible viscous fluid along with heat transfer due to an infinite rotating disk in a porous medium.

The above mentioned studies have ignored the combined effect of uniform magnetic field and Soret diffusion in a porous medium. This gap motivates us to take up the present work wherein we study the influence of a uniform magnetic field and Soret effects on steady, viscous incompressible flow of an electrically conducting

fluid along with heat and mass transfer due to a rotating disk embedded in a porous medium.

In order to understand the fluid properties, the effect of various non dimensional parameters on radial, tangential, axial velocities and temperature are calculated and plotted. The results obtained are validated for vanishing magnetic field and porosity parameter which are found to be in good agreement with the results obtained by Ostrach and Thornton (1958). In the present work, mass concentration is also taken into an account.

6.2. Flow Description and Governing Equations

We consider a steady, hydromagnetic axially symmetric, viscous incompressible fluid with heat and mass transfer due to a rotating disk embedded in a porous medium. A system of cylindrical polar coordinates (r, ϕ, z) is introduced. It is assumed that the disk rotate with constant angular velocity Ω and placed at $z = 0$. The fluid occupies the region $z > 0$, where z is the vertical axis in the cylindrical coordinates, r and ϕ are the radial and tangential axes respectively as indicated in figure 6.1.

The fluid velocity components are (u, v, w) in the direction of (r, ϕ, z) respectively. The surface of the rotating disk is maintained at a uniform temperature T_w. Far away from the surface, the free stream is kept at a constant temperature T_∞ and at a constant pressure p_∞. The external uniform magnetic field $\vec{B}_0$ is imposed in the direction normal to the surface of the disk. It is assumed that the induced magnetic field due to the motion of the electrically conducting fluid is negligible.

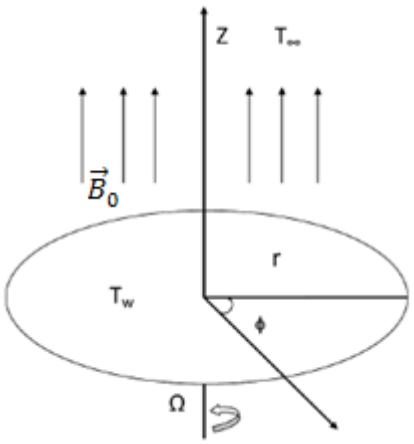

Fig 6.1 Schematic diagram of the problem

In the present work, the following assumptions are made:

- Flow of a Newtonian and electrically conducting fluid is considered which is steady, viscous, incompressible and laminar in nature.
- The fluid is infinite in extent in the positive z-direction.
- The disk rotates with constant angular velocity Ω and placed at $z = 0$.
- The surface of the rotating disk is maintained at a uniform temperature T_w.
- The external magnetic field $\vec{B}_0$ is imposed in the direction normal to the surface of the disk.
- Magnetic Reynolds number is considered small enough to neglect the induced magnetic field.

Under these assumptions, the governing equations for the continuity, momentum and energy in laminar incompressible flow can be written as follows:

$$\frac{\partial u}{\partial r} + \frac{u}{r} + \frac{\partial w}{\partial z} = 0 \tag{6.1}$$

$$u\frac{\partial u}{\partial r} - \frac{v^2}{r} + w\frac{\partial u}{\partial z} + \frac{1}{\rho}\frac{\partial p}{\partial r} = \gamma\left(\frac{\partial^2 u}{\partial r^2} + \frac{1}{r}\frac{\partial u}{\partial r} - \frac{u}{r^2} + \frac{\partial^2 u}{\partial z^2}\right) - \frac{\sigma B_0^2}{\rho}u - \frac{\gamma}{k}u \tag{6.2}$$

$$u\frac{\partial v}{\partial r} + \frac{uv}{r} + w\frac{\partial v}{\partial z} = \gamma\left(\frac{\partial^2 v}{\partial r^2} + \frac{1}{r}\frac{\partial v}{\partial r} - \frac{v}{r^2} + \frac{\partial^2 v}{\partial z^2}\right) - \frac{\sigma B_0^2}{\rho}v - \frac{\gamma}{k}v \tag{6.3}$$

$$u\frac{\partial w}{\partial r} + w\frac{\partial w}{\partial z} + \frac{1}{\rho}\frac{\partial p}{\partial z} = \gamma\left(\frac{\partial^2 w}{\partial r^2} + \frac{1}{r}\frac{\partial w}{\partial r} + \frac{\partial^2 w}{\partial z^2}\right) - \frac{\gamma}{k}w \tag{6.4}$$

$$u\frac{\partial T}{\partial r} + w\frac{\partial T}{\partial z} = \frac{\kappa}{\rho C_p}\left(\frac{\partial^2 T}{\partial r^2} + \frac{1}{r}\frac{\partial T}{\partial r} + \frac{\partial^2 T}{\partial z^2}\right) \tag{6.5}$$

$$u\frac{\partial C}{\partial r} + w\frac{\partial C}{\partial z} = D_M\left(\frac{\partial^2 C}{\partial r^2} + \frac{1}{r}\frac{\partial C}{\partial r} + \frac{\partial^2 C}{\partial z^2}\right) + D_T\left(\frac{\partial^2 T}{\partial r^2} + \frac{1}{r}\frac{\partial T}{\partial r} + \frac{\partial^2 T}{\partial z^2}\right) \tag{6.6}$$

The appropriate boundary conditions for velocity, temperature and mass concentration are given by

$$u = 0, \quad v = \Omega r, \; w = 0, \; T = T_w \,, C = C_w \text{ at } \; z = 0 \tag{6.7}$$

$$u \to 0, \; v \to 0, T \to T_\infty \,, \quad C \to C_\infty \text{ as } \quad z \to \infty \tag{6.8}$$

6.3. Solution of the Problem

We use similarity technique to solve the system of equations (6.1)-(6.6) along with the boundary conditions (6.7) and (6.8). Following Von Karman (1921), a dimensionless normal distance from the disk, $\eta = z\sqrt{\frac{\Omega}{\gamma}}$ is introduced with the following representations for the radial, tangential and axial velocities, pressure and temperature distributions.

$$u = \Omega r F(\eta),\ v = \Omega r G(\eta),\ w = (\Omega r)^{1/2} H(\eta),\ p - p_\infty = 2\mu\Omega P(\eta)$$

$$\theta(\eta) = \frac{T - T_\infty}{T_w - T_\infty}, \phi(\eta) = \frac{C - C_\infty}{(C_w - C_\infty)} \tag{6.9}$$

where T, C, μ, σ and $\gamma = (\mu/\rho)$ represent respectively the temperature, mass concentration, coefficient of viscosity, electrical conductivity and the kinematic viscosity of the fluid. . The constant parameters in the system: $k, C_p, \kappa,\ D_M$ and D_T respectively the permeability of porous material, specific heat at constant pressure, thermal conductivity of the fluid, molecular diffusivity and thermal diffusivity. F, G, H, θ, ϕ and P are non-dimensional functions in terms of vertical coordinate η.

Introducing the above transformations in equations (6.1)-(6.6), we obtain the system of ordinary differential equations,

$$2F + H' = 0, \tag{6.10}$$

$$F'' - HF' - F^2 + G^2 - MF - D_a F = 0, \tag{6.11}$$

$$G'' - HG' - 2FG - MG - D_a G = 0, \tag{6.12}$$

$$H'' - HH' - 2P' - D_a H = 0, \tag{6.13}$$

$$\theta'' - PrH\theta' = 0, \tag{6.14}$$

$$\phi'' - ScH\phi' + ScSr\theta'' = 0. \tag{6.15}$$

The transformed boundary conditions are given as,

$$F = 0,\ G = 1,\ H = 0,\ \theta = 1,\ \phi = 1 \text{ at } \eta = 0 \tag{6.16}$$

$$F \to 0, G \to 0, \theta \to 0, \phi \to 0 \text{ as } \eta \to \infty \tag{6.17}$$

where $M = \frac{\sigma B_0^2}{\rho\Omega}$ is the magnetic parameter, $Pr = \mu C_p/\kappa$ is the Prandtl number, $Sc = \frac{\gamma}{D_m}$ is the Schmidt number, $Sr = \frac{(T_w - T_\infty)D_T}{(C_w - C_\infty)\gamma}$ is the Soret number and $D_a = \frac{\gamma}{K\Omega}$ is the local Darcy number.

The non-linear coupled ordinary differential equations (6.10)-(6.12) and (6.14)-(6.15) subject to boundary conditions (6.16) and (6.17) are reduced to a system of first order ordinary differential equations as follows,

$$F' = w,\ \theta = y,\ \theta' = z,\ \phi = b,\ \phi' = e, G = i, G' = a, H = c$$

$$c' = -2x \tag{6.18}$$

$$w' = cw + x^2 - i^2 + Mx + D_a x \tag{6.19}$$

$$a' = ca + 2xi + Mi + D_a i \tag{6.20}$$

$$z' = Prcz, \tag{6.21}$$

$$e' = Scce - ScSrPrcz \tag{6.22}$$

and boundary conditions become,

$x(0) = 0,\ \ i(0) = 1,\ \ c(0) = 0,\ \ y(0) = 1,\ \ b(0) = 1$ at $\eta = 0$ (6.23)

$x \to 0, i \to 0, y(0) \to 0,\ \ b(0) \to 0$ as $\eta \to \infty$ (6.24)

We have solved the equations (6.18)-(6.22) with boundary conditions (6.23) and (6.24) using shooting method.

The major physical quantities - skin-friction coefficient C_f , the local Nusselt number Nu_x, and the local Sherwood number Sh_x are defined respectively as follows: The radial shear stress and tangential shear stress are given by,

$$\tau_r = \left[\mu\left(\frac{\partial u}{\partial z}\right) + \left(\frac{\partial w}{\partial r}\right)\right]_{z=0} = \mu(Re)^{\frac{1}{2}}\Omega F'(0)$$

$$\tau_t = \left[\mu\left(\frac{\partial v}{\partial z}\right)\right]_{z=0} = \mu(Re)^{\frac{1}{2}}\Omega G'(0)$$

Hence the radial and tangential skin-frictions are,

$$F'(0) = (Re)^{\frac{1}{2}}C_{fr}$$

$$G'(0) = (Re)^{\frac{1}{2}}C_{ft}$$

Rate of heat transfer and the rate of mass transfer are given by,

$$q_w = -k\left[\frac{\partial T}{\partial z}\right]_{z=0} = -k(T_w - T_\infty)\left(\frac{\Omega}{\nu}\right)^{\frac{1}{2}}\theta'(0)$$

$$m_w = -D\left[\frac{\partial C}{\partial z}\right]_{z=0} = -D(C_w - C_\infty)\left(\frac{\Omega}{\nu}\right)^{\frac{1}{2}}\phi'(0)$$

Hence the Nusselt number (Nu_x) and the Sherwood number (Sh_x) are obtained as,

$$(Re)^{\frac{1}{2}}Nu_x = -\theta'(0)$$

$$(Re)^{\frac{1}{2}}Sh_x = -\phi'(0)$$

where $Re = \frac{\Omega r^2}{\gamma}$ is the rotational Reynolds number.

6.4. Results and Discussion

In order to get physical insight of the problem we have studied velocity, temperature and concentration profiles as a function of various parameters such as magnetic parameter M, Schmidt number Sc, Soret number Sr, Darcy number D_a. The effect of flow parameters on velocity field, skin-friction, Nusselt number and Sherwood number are calculated numerically and discussed with the help of graphs.

We have shown the effect of velocities - radial, tangential and axial, temperature through figures (6.2) and (6.3) for vanishing magnetic field and porosity

parameter. It can be seen from these figures that our results are in good agreement with Ostrach and Thornton (1958).

Figures (6.4)-(6.8) show the effect of magnetic field M on radial, tangential, axial components of velocities i.e., $F(\eta), G(\eta)$ and $H(\eta)$, temperature $\theta(\eta)$ and concentration $\phi(\eta)$ respectively. Radial and tangential velocities decrease when magnetic field increases, whereas the axial velocity increases, when magnetic field increases. We also observe that temperature and concentration increase, when magnetic field increases. However, the effect of the magnetic field on the concentration distribution is not very significant. It is evident from these figures that an increase in the magnetic parameter depreciates velocity and enhances the temperature and concentration profiles. We can observe that the enhancement of Lorentz force slows down the motion of an electrically conducting fluid.

Figures (6.9) and (6.10) exhibit the effect of Schmidt number Sc and Soret number Sr on concentration profiles. These two figures illustrate that the increase in Schmidt number Sc and Soret number Sr causes the decrease and increase in concentration profiles respectively.

Figures (6.11)-(6.15) exhibit the effect of Darcy number on radial, tangential and axial components of velocities, $F(\eta), G(\eta)$ and $H(\eta)$, temperature $\theta(\eta)$ and concentration $\phi(\eta)$. It can be inferred from these graphs that increase in Darcy number results in enhancement of axial velocity, temperature and mass concentration while, radial and tangential velocity components decrease due to the increase of Darcy number.

Figures (6.16)-(6.19) depict the axial skin-friction $F'(0)$, tangential skin-friction $G'(0)$, the rate of heat transfer $\theta'(0)$ and the rate of mass transfer $\phi'(0)$ as a function of Darcy number D_a for various values of M. We observe that the axial skin-friction $F'(0)$ and tangential skin-friction $G'(0)$ decrease due to increase in Darcy number D_a and magnetic parameter M. Figures (6.18) and (6.19) show that increasing Darcy number D_a and magnetic parameter M increase the rate of heat transfer and decrease the rate of mass transfer.

6.5. Conclusion

The effect of uniform magnetic field on the steady free convective viscous incompressible flow of an electrically conducting fluid along with heat and mass transfer due to a rotating disk embedded in a porous medium has been investigated. The non-linear boundary layer equations together with the boundary conditions are reduced to a system of non-linear ordinary differential equations by using the Von Karman similarity transformation. The system of non-linear ordinary differential equations is solved by shooting procedure using fourth order Runge-Kutta Method. Effect of various non-dimensional parameters on the fluid flow, heat and mass transfer characteristics are examined.

The following conclusions are drawn from the present study:

- Radial and tangential velocities decrease when magnetic field increases, whereas the axial velocity increases, when magnetic field increases.
- The temperature and the concentration fields increase, when magnetic field increases. However, the effect of the magnetic field on the concentration distribution is not very significant.
- The increase in Schmidt number Sc and Soret number Sr causes an increase in concentration profiles.
- The axial skin-friction $F'(0)$ and tangential skin-friction $G'(0)$ decrease due to increase in Darcy number D_a and magnetic parameter.
- Increasing Darcy number and magnetic parameter increase the rate of heat transfer and decrease the rate of mass transfer.

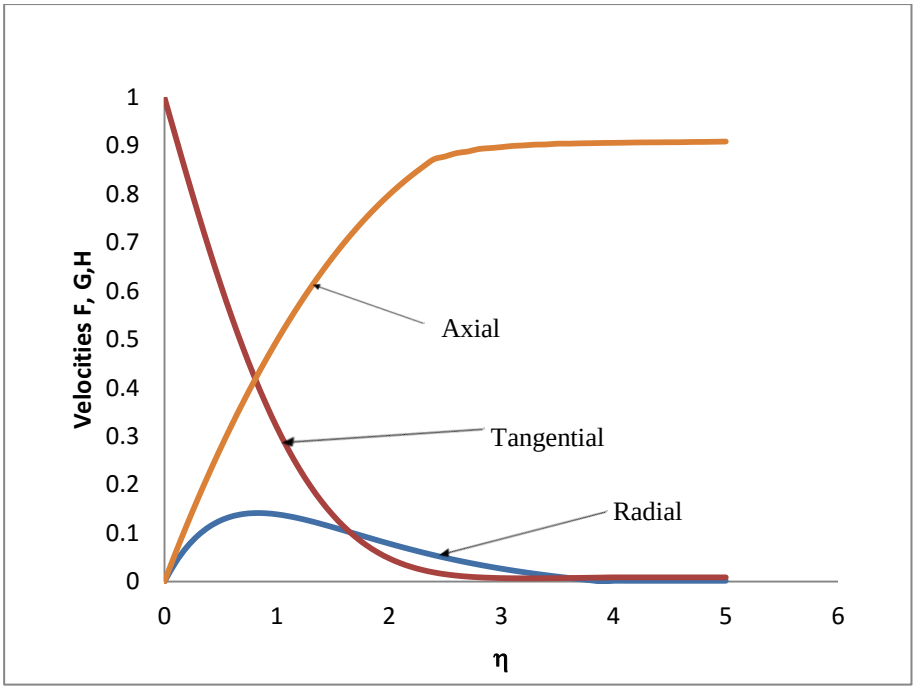

Fig 6.2 Velocity functions; Pr=7.0; M=0.0; k=0.0*

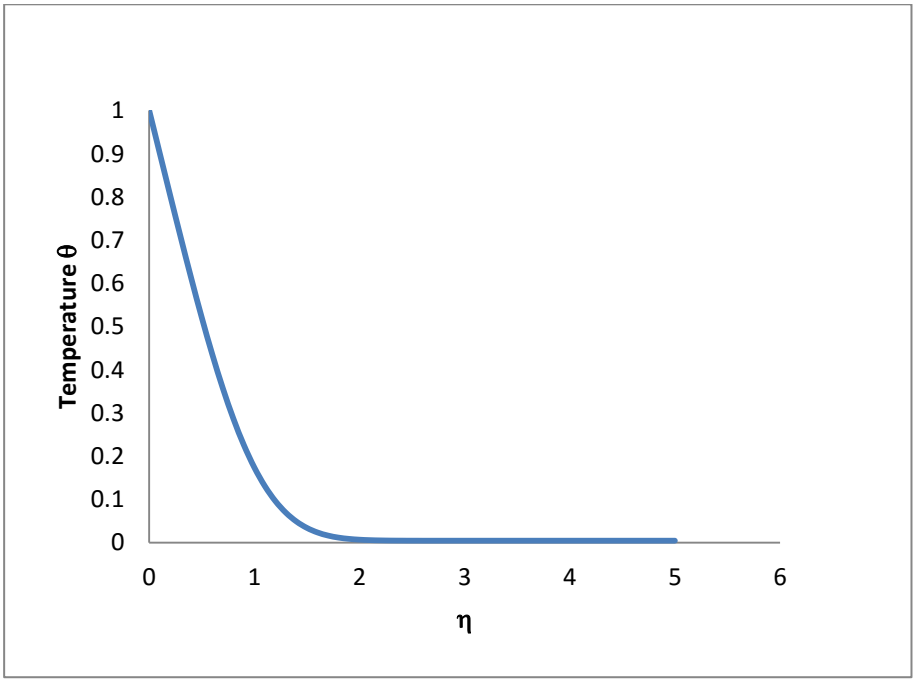

Fig 6.3 Temperature distribution; Pr=7.0; M=0.0; k=0.0*

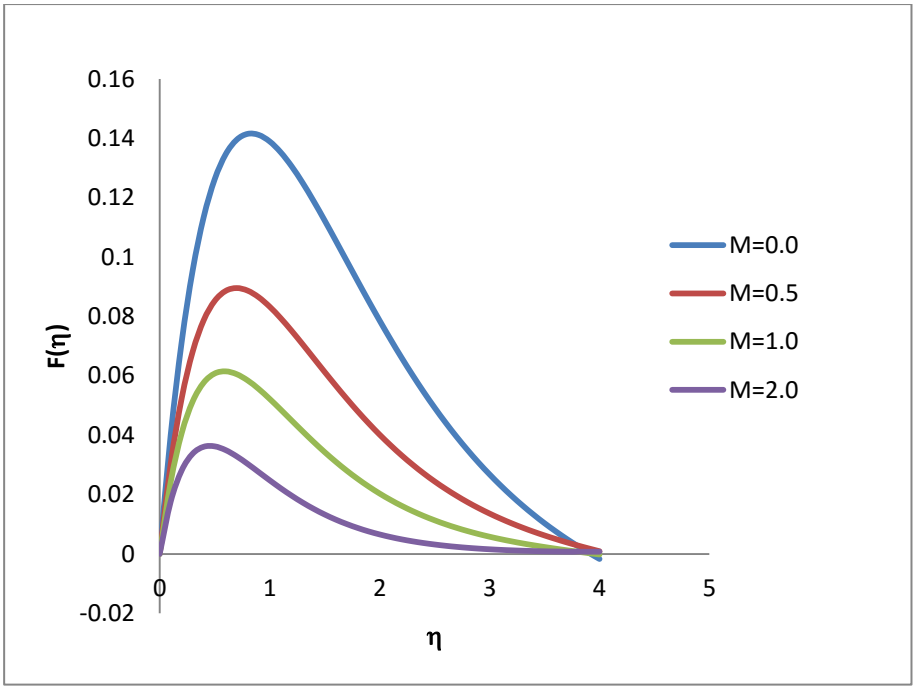

Fig 6.4 Radial velocity $F(\eta)$ for various values of M; Pr=7.0; Sc=0.3; Sr=0.3; D_a=0.2

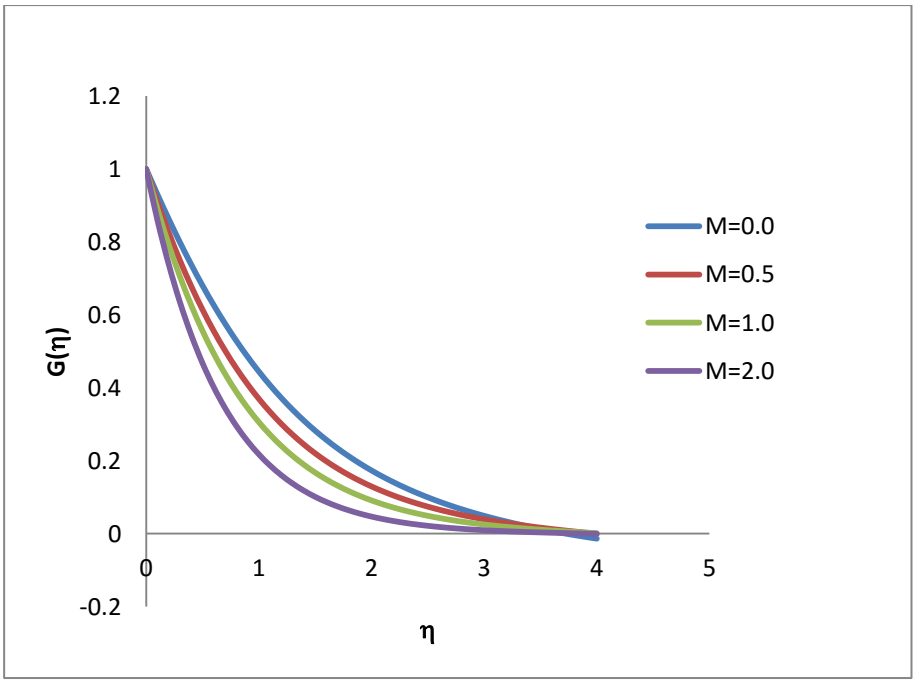

Fig 6.5 Tangential velocity $G(\eta)$ for various values of M; Pr=7.0; Sc=0.3; Sr=0.3; D_a=0.2

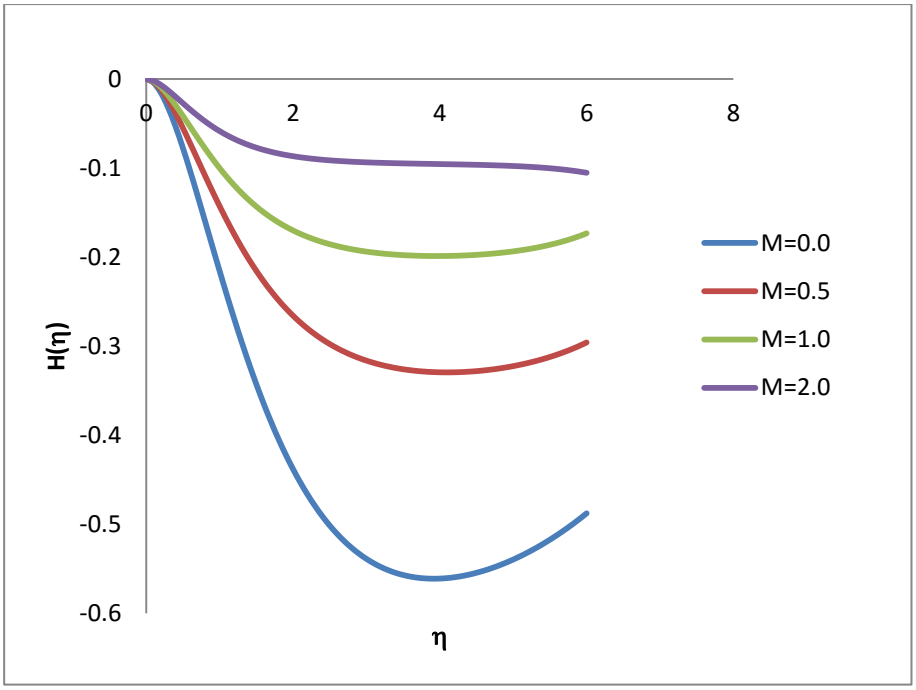

Fig 6.6 Axial velocity $H(\eta)$ for various values of M; Pr=7.0; Sc=0.3; Sr=0.3; D_a=0.2

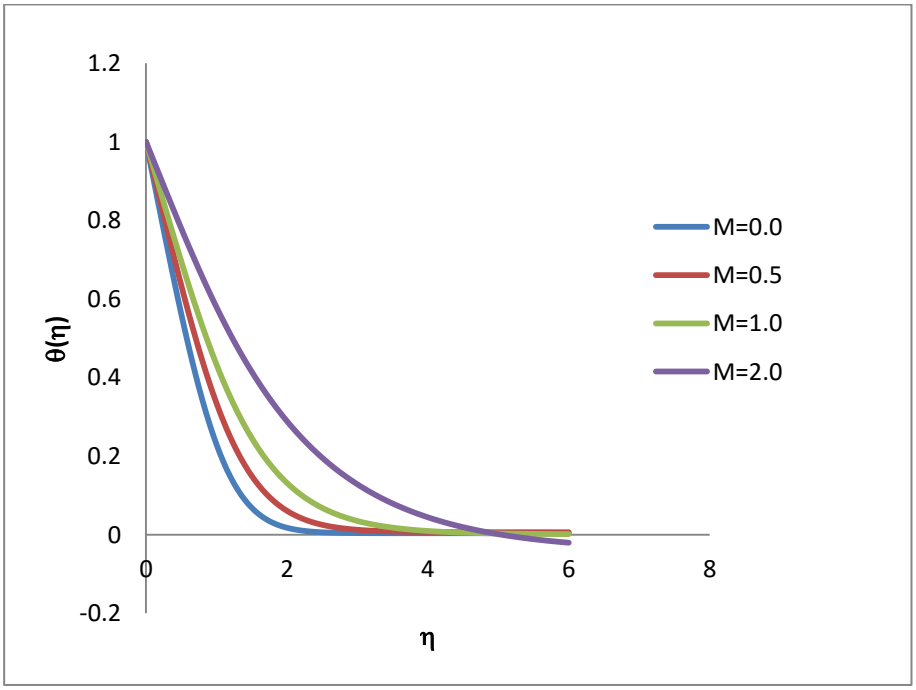

Fig 6.7 Temperature $\theta(\eta)$ for various values of M; Pr=7.0; Sc=0.3; Sr=0.3; D_a=0.2

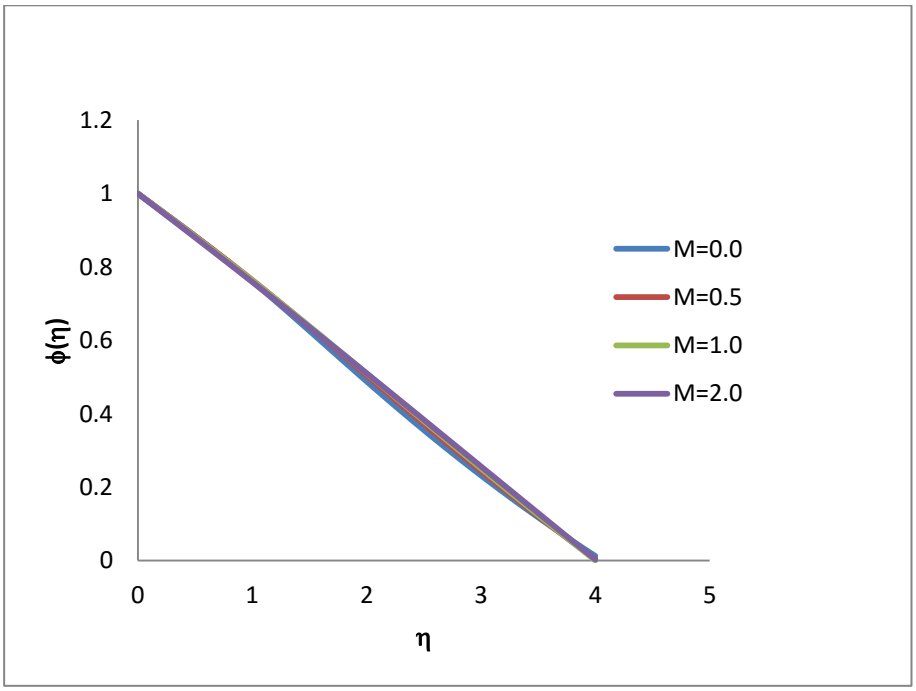

Fig 6.8 Concentration profiles $\phi(\eta)$ for various values of M; Pr=7.0; Sc=0.3; Sr=0.3; D_a=0.2

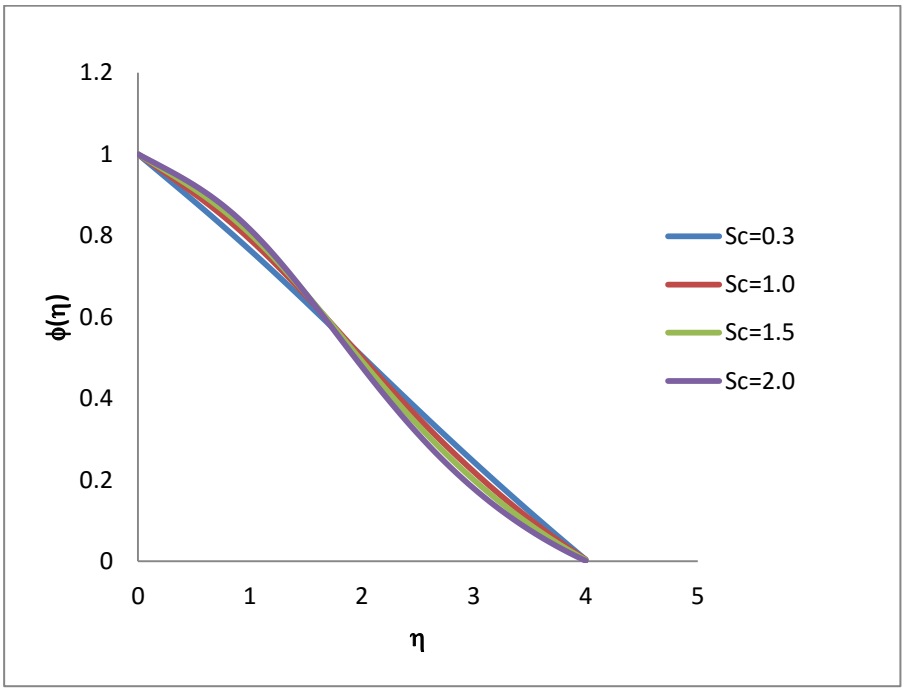

Fig 6.9 Concentration $\phi(\eta)$ for various values of Sc; Pr=7.0; M=0.5; Sr=0.3; D_a=0.2

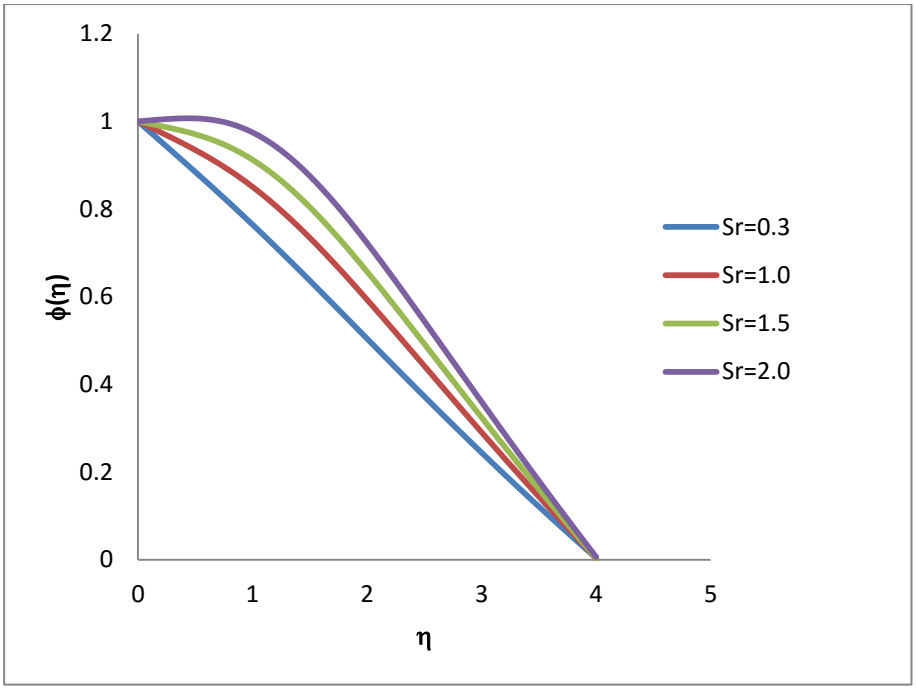

Fig 6.10 Concentration $\phi(\eta)$ for various values Sr; Pr=7.0; Sr=0.3; M = 0.5; D_a=0.2

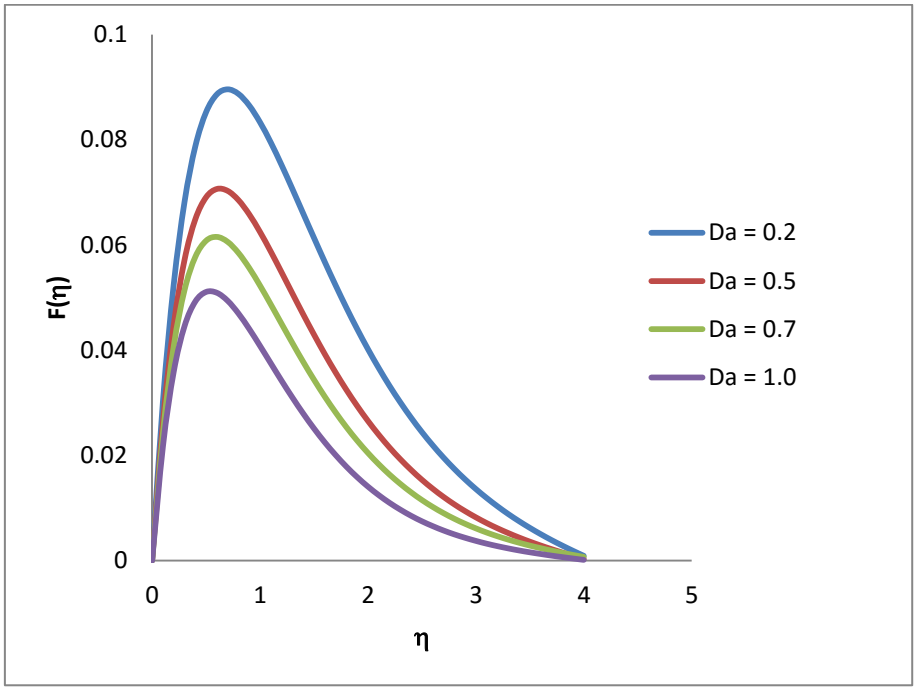

Fig 6.11 Radial velocity $F(\eta)$ for various values D_a; Pr=7.0; Sr=0.3; Sc=0.3; M = 0.5

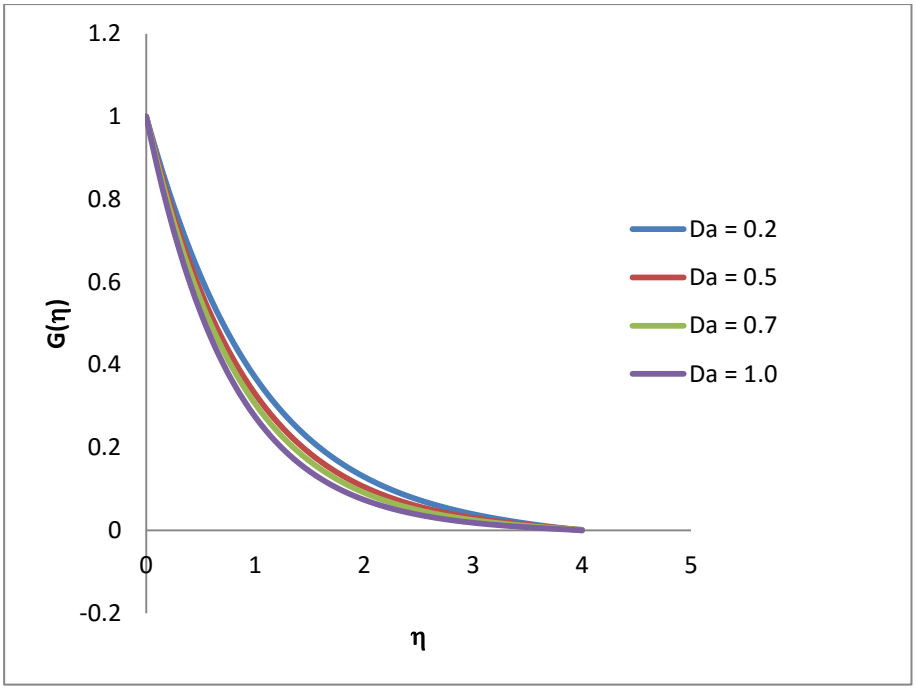

Fig 6.12 Tangential velocity $G(\eta)$ for various values of D_a; Pr=7.0; Sr=0.3; Sc=0.3; M = 0.5

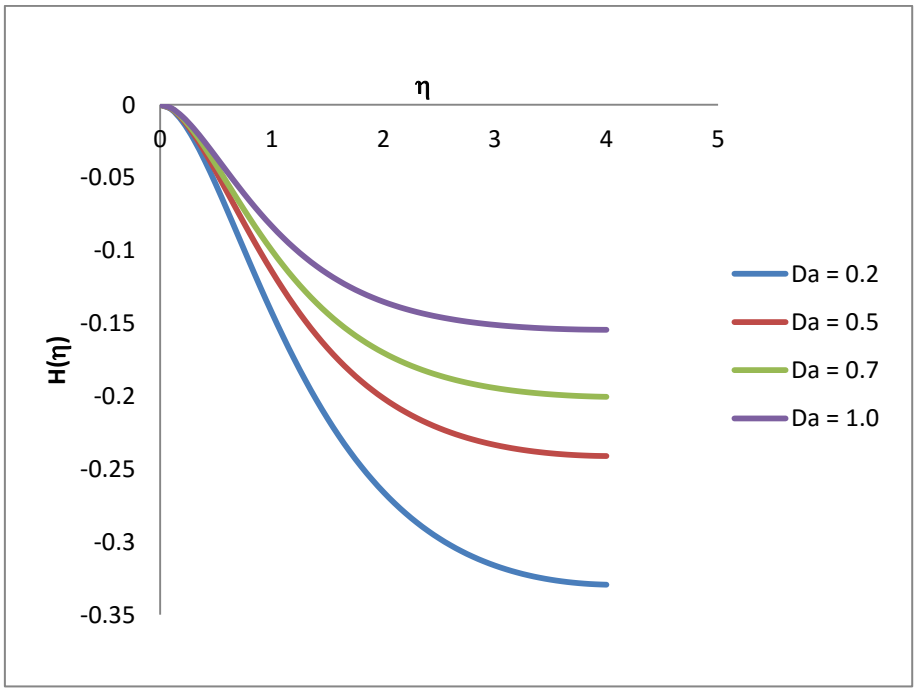

Fig 6.13 Axial velocity $H(\eta)$ for various values of D_a; Pr=7.0; Sr=0.3; Sc=0.3; M = 0.5

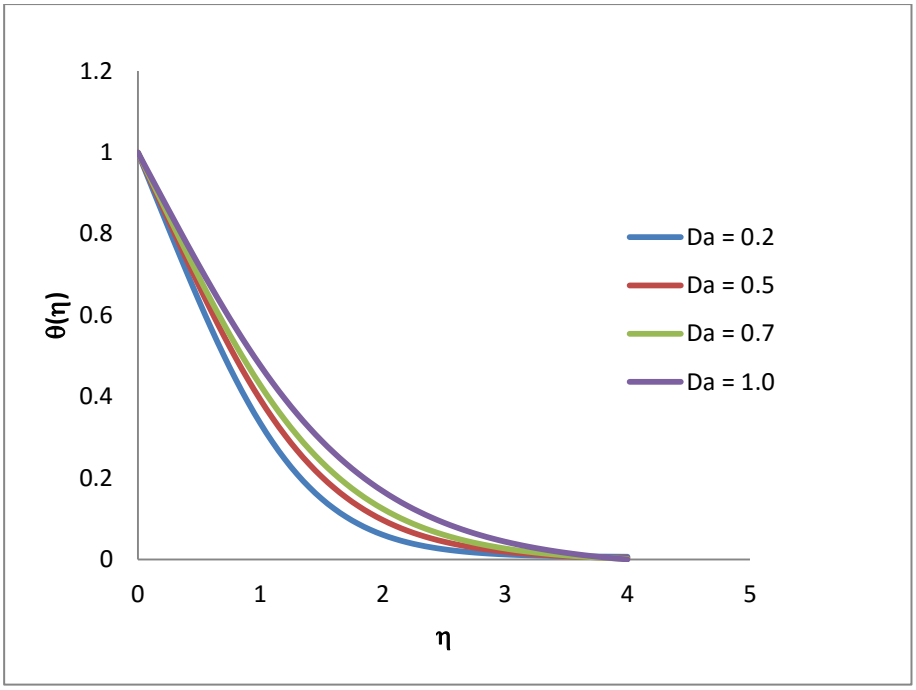

Fig 6.14 Temperature $\theta(\eta)$ for various values of D_a; Pr=7.0; Sr=0.3; Sc=0.3; M = 0.5

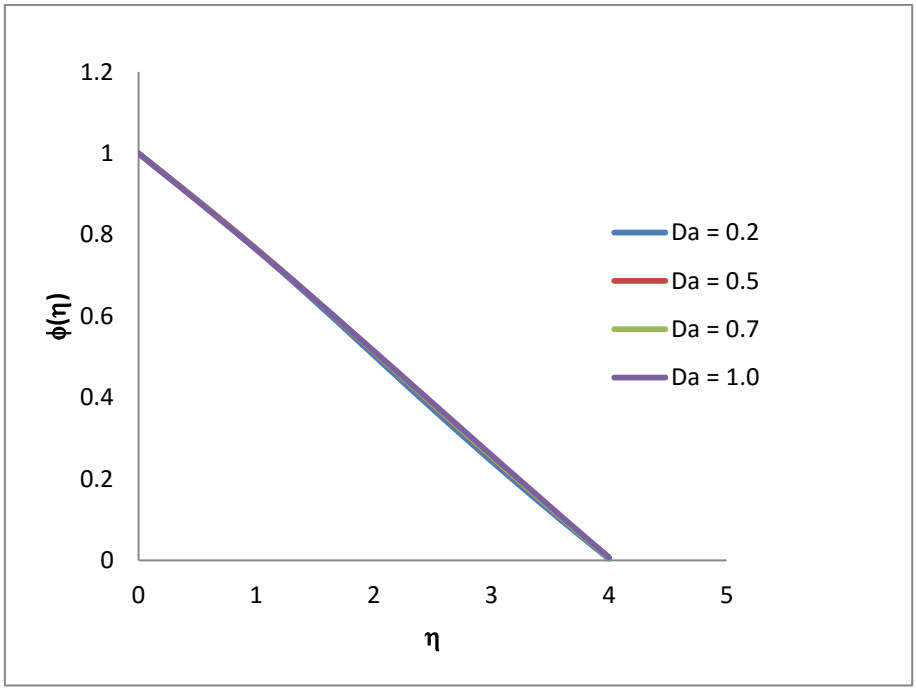

Fig 6.15 Concentration $\phi(\eta)$ for various values of D_a; Pr=7.0; Sr=0.3; Sc=0.3; M = 0.5

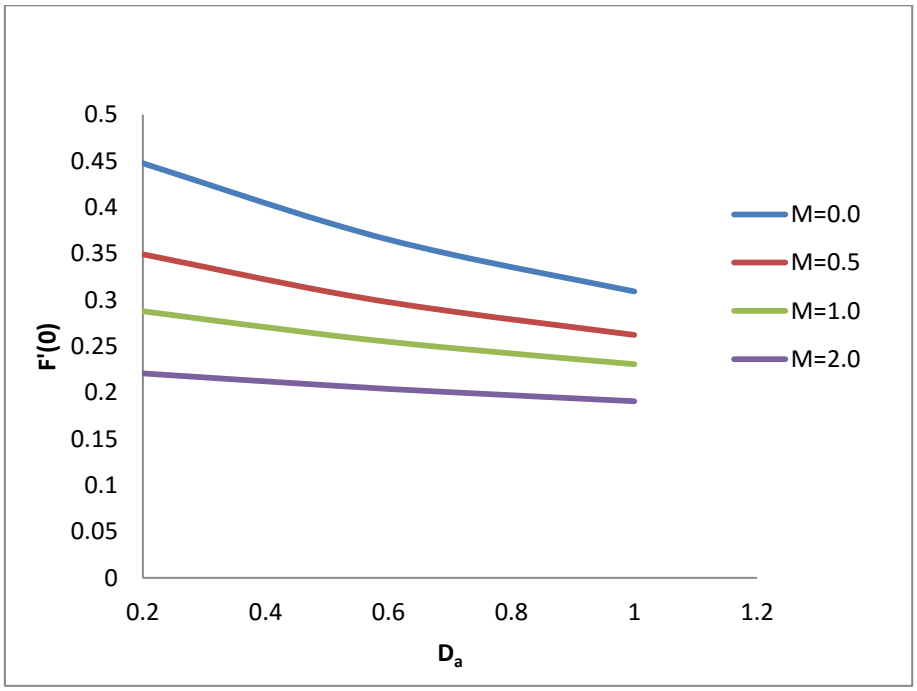

Fig 6.16 Axial skin-friction $F'(0)$ against D_a for various values of M; Pr=7.0; Sc=0.3; Sr=0.3

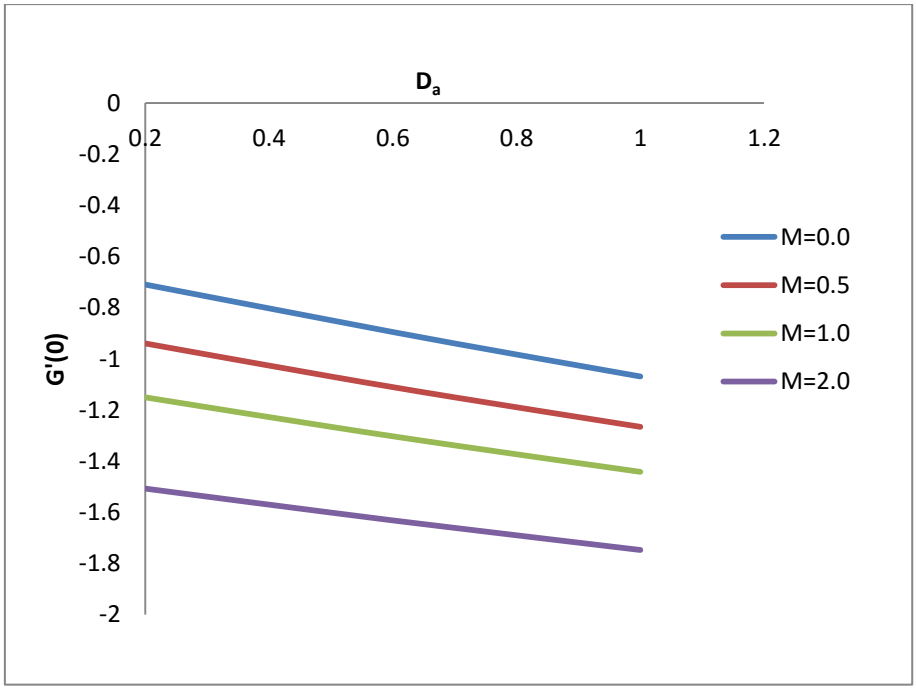

Fig 6.17 Tangential skin-friction $G'(0)$ against D_a for various values of M; Pr=7.0; Sc=0.3; Sr=0.3

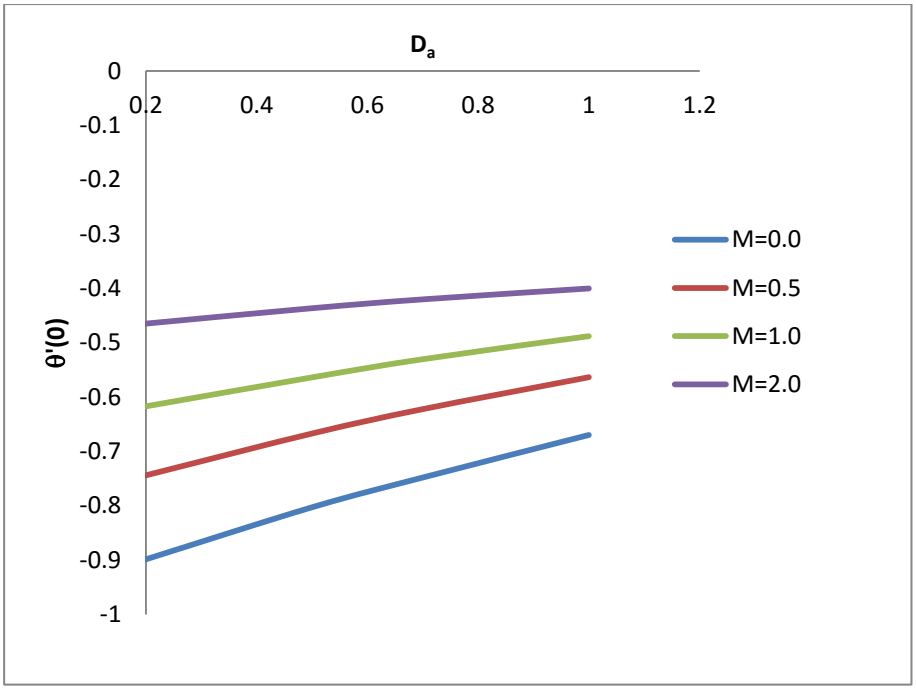

Fig 6.18 Rate of heat transfer $\theta'(0)$ against D_a for various values of M; Pr=7.0; Sc=0.3; Sr=0.3

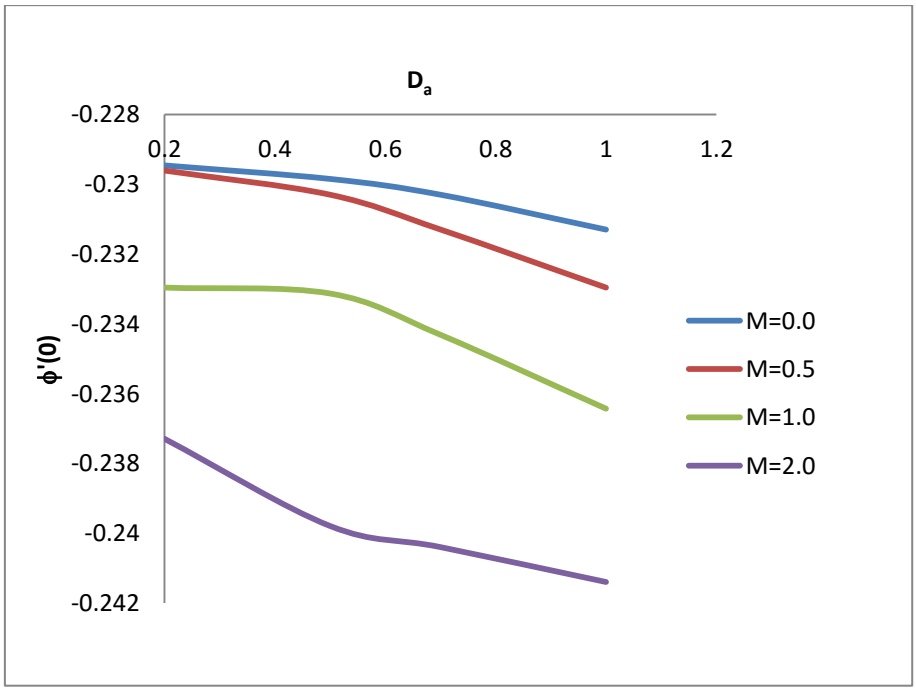

Fig 6.19 Rate of mass transfer $\phi'(0)$ against D_a for various values of M; Pr=7.0; Sc=0.3; Sr=0.3